Diyala Journal of Engineering Sciences

Journal homepage: https://djes.info/index.php/djes

ISSN: 1999-8716 (Print); 2616-6909 (Online)

# Structural Behaviour of Reinforced Reactive Powder Concrete One Way Slab

Tahseen A. Madhloom[1*], Murtada A. Ismael[2]

[1] Department of Civil Engineering, University of Diyala, 32001 Diyala, Iraq
[2] Department of Highway and Airport Engineering, University of Diyala, Diyala, Iraq

**ARTICLE INFO**

***Article history:***
Received March 14, 2024
Revised May 24, 2024
Accepted June 2, 2024
Available online June 5, 2024

***Keywords:***
Structural behavior
Reactive powder concrete
One-way slab
Steel fiber
Slab thickness

**ABSTRACT**

Reactive powder concrete (RPC) is advanced cement-based material that has been enhanced and improved in recent decades which showing superior performance on structural systems. This paper shows experimental research to study the structural performance of reactive powder reinforced concrete one-way slabs in static loading by applying two symmetric loads and simply support type. In the present investigation, five RPC one-way slabs designed, casted and tested. All the slabs were similar in the length and the width (980x400mm), also in the properties of materials and their proportions, but different in thickness and the ratios of main reinforcement. They were cast into two groups; the first group had three values of longitudinal reinforcement proportions (ρ): 0.0036, 0.0048, and 0.0060, respectively, and the second group included three values of slab thickness: 40 mm, 60 mm, and 80 mm, respectively. Experimentally, it has been noticed that the ductility and flexural behaviour of RPC one-way slabs are considerably affected by increasing slab thickness but influence of longitudinal reinforcement less significant. The results of specimen testing indicated that increasing main steel reinforcement proportion from 0.0036 to 0.0048 and to 0.0060 led to an increase in the first cracking load test with a value of (19%, 43%), respectively, an increase in the ultimate load test with a value of (21%, 40.91%) respectively, and the value of ultimate mid-span deflection increased from 17.78% to 28.98%. The test results also revealed that the increase in thickness of slabs from 40mm to 60mm and then to 80mm led to an increase in the first cracking load test with a value of (166%, 240%), respectively, increase the ultimate load by (104.06%, 234.71%), respectively, and the value of ultimate mid-span deflection decreased from 36.82% to 58.26.

## 1. Introduction

Reinforced concrete solid slabs are one of the most common fundamental components used in a wide range of engineering structures and applications. Reactive powder reinforced concrete is considered one of the important improvements in concrete technology, exhibiting superior properties such as high durability, great ductility, high strength, and long-term stability. Reactive powder concrete is as well Known as ultrahigh high-performance concrete (UHPC) because of its excellent structural behavior. RPC consists of a significant amount of cement mixture with silica fume, fine sand of particles less than 600 μm in size, steel fiber (of different types, sizes, and geometries), superplasticizer, a low water cement ratio (less than 0.2) and the absence of coarse aggregates. RPC can reach remarkable values for absorption of energy that are close to those of metals due to the high ductility that

* Corresponding author.
E-mail address: tahseenam79@gmail.com
DOI: 10.24237/djes.2024.17203

characterizes it. It is possible to use RPC in many structural element types. The first structural construction project utilizing RPC was the Sherbrooke footbridge in Canada, finished through the year 1997 [1-6]. Many research works have been done to study the performance of reinforced concrete one-way slabs, some of these researches deal with using GFRP bars or CFRP bars instead of steel bars as the main reinforcement of slabs to research their behavior on flexural of one-way slabs [7-10]. Aljazaeri and Myers (2018) showed that the flexural strength of RC one-way slabs improved by strengthening with fiber-reinforced cementitious matrix (FRCM), carbon-fiber-reinforced polymer (CFRP), and steel-reinforced polymer (SRP) composites [11]. Yoo and Yoon (2014) revealed that increasing the maximum impact load and dissipating energy before failure and the impact resistance of the steel fiber-reinforced concrete slabs were substantially improved by using externally strengthening the fiber-reinforced polymer sheets [12]. Elsanadedy, Almusallam et al. (2015) indicated that the externally bonded fiber reinforced polymer (FRP) composite systems are effective in upgrading the flexural capacity and stiffness of RC one-way slabs but with the reduction of their deflection ductility [13]. Allawi and Jabir (2016) showed that increasing the lacing steel ratio enhanced the ultimate load capacity, significant improvements in ductility, and decreased the span to effective depth ratio with respect to the control specimen [14]. Adom-Asamoah and Kankam (2009) revealed that the failure modes of one-way concrete slabs were either one or a combination of modes of tension failure, concrete crushing, diagonal shear, or shear bond failures [15]. Baarimah and Mohsin (2017) indicated that there was a promising improvement in the load-carrying capacity and ductility as well as a delay in crack propagation for the slabs with Vf = 2%, and the addition of fibers compensated for the reduction in the slab thickness as well as changed the failure mode of the slab from brittle to a more ductile manner [16]. Kumari, Puttappa et al. (2013) showed that the ultimate load capacity of steel fiber reinforced self-compacting concrete (SFRSCC) and steel fiber reinforced normal concrete (SFRNC) slabs calculated using ACI-318 is an under estimation of ultimate load with a range of 18–32% compared to the experimental ultimate load, and the ratio of calculated deflection to experimental deflection was 0.94 for ACI-318 [17]. Ahmed (2018) reported that the ultimate load capacity of reinforced concrete slabs with openings is less than that of reinforced concrete one-way slabs without openings. The service deflection, concrete compressive strain, and crack width of reinforced concrete slabs with openings are greater than those of reinforced concrete one-way slabs without openings [18]. Many researchers investigated the effect of characteristics of shear in the case of longitudinal reinforcement spacing and closed the concentrated load to support [19-20]. Very few studies deal with the behavior of one-way slabs that pour using reactive powder concrete. Qasim (2013) studied the opening effect on the flexural performance of reinforced reactive powder concrete one-way slabs, the results revealed to: Adding steel fibers and silica fume to the mixture results in an increase in ultimate load. The ultimate load is significantly decreased in slabs with square openings (100, 150, and 200mm) when compared to the corresponding solid slabs. Increasing the percentage of steel fibers in RPC slabs results in a significant reduction in crack width and increasing the volumetric ratio of steel fiber resulted in an increase the ultimate concrete strain at both compression and tension regions [21]. Alfeehan, Abdulkareem et al. (2017) investigated the flexural behavior of sustainable RPC one-way slab with bubbles for flooring elements, the obtained results indicated that: Increasing the proportion of steel fibers enhanced the ultimate load for bubbled slabs that reinforce in the top and bottom directions and a decrease of the deflection. The ultimate load capacity increased for bubbled slabs that reinforced in the top and bottom directions by increasing the thickness of the slab from 100 to 125 mm. The saving of concrete in bubble slabs was 18% compared to the solid slab, and the bubble slabs achieve the requirements of sustainability [22]. Abtan and Hassan (2019) studied the flexural strength of modified reinforced reactive powder concrete (MRPC) one-way slabs, the result showed that: An improvement in the ultimate load was achieved for modified reactive powder concrete slabs when increasing the thickness of the slab, adding the steel fibers with a proportion of (0.4%, 0.8%) to the concrete mixture of the MRPC slabs enhanced the ultimate load capacity, increased the ductility of MRPC slabs, improved their stiffness, reduced the rate of propagation of cracks, and reduces the width of cracks [23]. From the previous studies which dealt with the field of the structural behavior of reactive powder reinforced concrete one-way slab, it can be noted that most of these studies focused on investigating the effect of opening in RPC one-way slabs, sustainable flooring elements of RPC bubbled slabs, modified reactive powder concrete one-way slabs, and some other parameters, but did not focus on the behavior of RPC one-way solid slabs, which is one of the fields that require study because, until this time, no research has dealt with this field and there is a lack of information about the analysis and design of RPC one-way solid slabs. Therefore, this research aims to present an experimental study on the structural behavior of a simply supported RPC one-way slab under static load to investigate the effects of the most important parameters such as concrete compressive strength, tensile steel reinforcement ratio, steel fiber volumetric ratio, and slab thickness.

## 2. Methodology

### *2.1. Experimental program*

The experimental work of the present investigation consists of five one-way slabs that were poured and tested under two-point loads. Slabs were designed with a suitable size in a way that was easy to fabricate, handle, test, and fail in flexural mode. The tested slabs are classified into two groups: the first one includes identical slabs with 980mm length, 400mm width, and 40mm thickness, but they are different in steel reinforcement ratios (ρ) of (0.36%, 0.48%, and 0.6%) and the second one involves slabs with the same length and width of 980mm x 400mm but different thicknesses of 40mm, 60mm, and 80mm. The steel bars used in the slabs had a 4mm diameter placed at the bottom face of the long direction of the slabs; the distance between bars in the short direction was 150mm. The concrete cover for steel bars is equal to 10 mm, and the effective depth is 26 mm for all slabs. Details of the longitudinal and cross-sections of the control specimen are shown in Figure 1.

### *2.2. Materials*

#### *2.2.1. Cement*

Ordinary Portland cement (CEM I) has been used in this research work to cast all specimens from the Sulaymaniyah cement factory in Iraq with the trade mark (Baziani). The test results of the physical properties and chemical composition of this type of cement are shown in Tables 1 and 2, which are in accordance with Iraqi standard specification No. 5/2019 [24].

#### *2.2.2. Fine sand*

The aggregate utilized in this work was very fine sand with a maximum particle size of 600 μm (0.6mm). This type was separated by sieving; its grading is shown in Table 3, which confirms the requirements of Iraqi standard specification No. 45/1984 [25].

#### *2.2.3. Mineral admixture silica fume*

A grey, extremely highly dense fine powder manufactured by (CONMIX Company) was used as a mineral admixture in this research work. The size of silica fume particles is less than the size of cement particles by 100 times. The test results of the chemical analysis and physical characteristics of silica fume are shown in Tables 4 and 5, which satisfy the requirements of ASTM C1240-04 [26].

#### *2.2.4. Chemical admixture superplasticizer*

High-performance concrete superplasticizer (as well recognized as High Range Water Reduction Agent HRWRA) depended on modified polycarboxylic ether. MasterGlenium 51 (formerly known as Glenium 51) doesn't contain chlorides and achieves the ASTM C494 requirements for types A and F [27].

### *2.2.5. Steel fibers*

Steel fibers were utilized through present work manufactured by (Hongtu Company Ltd., China) (length = 13mm, diameter = 0.25mm, aspect ratio L/D = 52, tensile strength = 2850 MPa, density = 7800 kg/m3, cross section = circular) and satisfies the requirements of ASTM A820/A 820M-2004 [28].

### *2.2.6. Water*

The water that was utilized for casting the mixes and curing the concrete specimens was tap water.

### *2.2.7. Steel reinforcement*

One size of deformed reinforcement bars with a diameter of 4 mm and a yield stress of 549 MPa complies with ASTM A615/615M-05 [29] and is used as the main reinforcing bar, which is located in the region of tension face of slab.

**Table 1:** Physical Properties * of Cement

| Physical Properties | Test Results | Iraqi specification / No. 5/2019 |
|---|---|---|
| Fineness using Blaine air permeability Apparatus ($m^2$ /kg) | 406 | 250 (Minimum) |
| Soundness using autoclave method | Not available | 0.8% (Maximum) |
| Setting time using Vicat's apparatus | | |
| Initial (min.) | 137 | 45 (Minimum) |
| Final (hr.) | 3:28 | 10 (Maximum) |
| Compressive strength for cement paste Cube (70.7 mm) at: | | |
| 3 days (MPa) | 24.7 | 15 (Minimum) |
| 7 days (MPa) | 32.5 | 23 (Minimum) |

* Physical tests were done by National Centre of Construction Laboratories

**Table 2:** Chemical composition * of cement

| Compound Composition | Chemical Composition | Weight (%) | Iraqi specification / No. 5/2019 |
|---|---|---|---|
| Lime | CaO | 61.17 | 50 (Minimum) |
| Silica | $SiO_2$ | 21.46 | |
| Alumina | $Al_2O_3$ | 4.14 | - |
| Iron oxide | $Fe_2O_3$ | 3.69 | - |
| Magnesia | MgO | 2.32 | 5.0 (Maximum) |
| Sulfate | $SO_3$ | 2.67 | 2.8 (Maximum) |
| Loss on ignition | L.O.I. | 2.36 | 4.0 (Maximum) |
| Insoluble residue | I.R. | 1.17 | 1.5 (Maximum) |
| Lime saturation factor | L.S.F. | 0.85 | (0.66-1.02) % |
| Tricalcium Silicate | $C_3S$ | 42.72 | - |
| Dicalcium Silicate | $C_2S$ | 29.25 | - |
| Tricalcium Aluminate | $C_3A$ | 5.65 | - |
| Tetra calcium alumina ferrite | $C_4AF$ | 11.21 | - |

* Chemical tests were done by National Centre of Construction Laboratories

**Table 3:** Grading of very fine sand

| Sieve Size (mm) | Cumulative Passing % | Iraqi Specification No.45/1984 |
|---|---|---|
| 4.75 | 100 | 95-100 |
| 2.36 | 100 | 95-100 |
| 1.18 | 100 | 90-100 |
| 0.60 | 100 | 80-100 |
| 0.30 | 33 | 15-50 |
| 0.15 | 8 | 0-15 |

**Table 4:** Chemical characteristics of silica fume

| Composition | Abbreviation | Content (%) | Specification Requirement (ASTM C 1240-04) |
|---|---|---|---|
| Silica | $SiO_2$ | 95.83 | 85.0 (Minimum) |
| Alumina | $Al_2O_3$ | 1.21 | - |
| Iron Oxide | $Fe_2O_3$ | 0.07 | - |
| Lime | CaO | 0.25 | - |
| Magnesia | MgO | 0.02 | - |
| Sulfate | $SO_3$ | 0.27 | - |
| Potassium Oxide | $K_2O$ | 0.49 | - |
| Moisture Content | $H_2O$ | - | 3.0 (Maximum) |
| Loss on Ignition | L.O.I. | 2.85 | 6.0 (Maximum) |

**Table 5:** Physical characteristics of silica fume

| Physical Characteristics | Silica Fume Analysis | Specification Requirement (ASTM C 1240) |
|---|---|---|
| Specific Surface Area ($m^2/g$) | 21 | 15 (Minimum) |
| Pozzolanic Activity Index, 7 days (%) | 129 | 105 (Minimum) |
| Over size particles retained on 45μm sieve | 7 | 10 (maximum) |
| Specific Gravity | 2.27 | 2.10 to 2.40 |

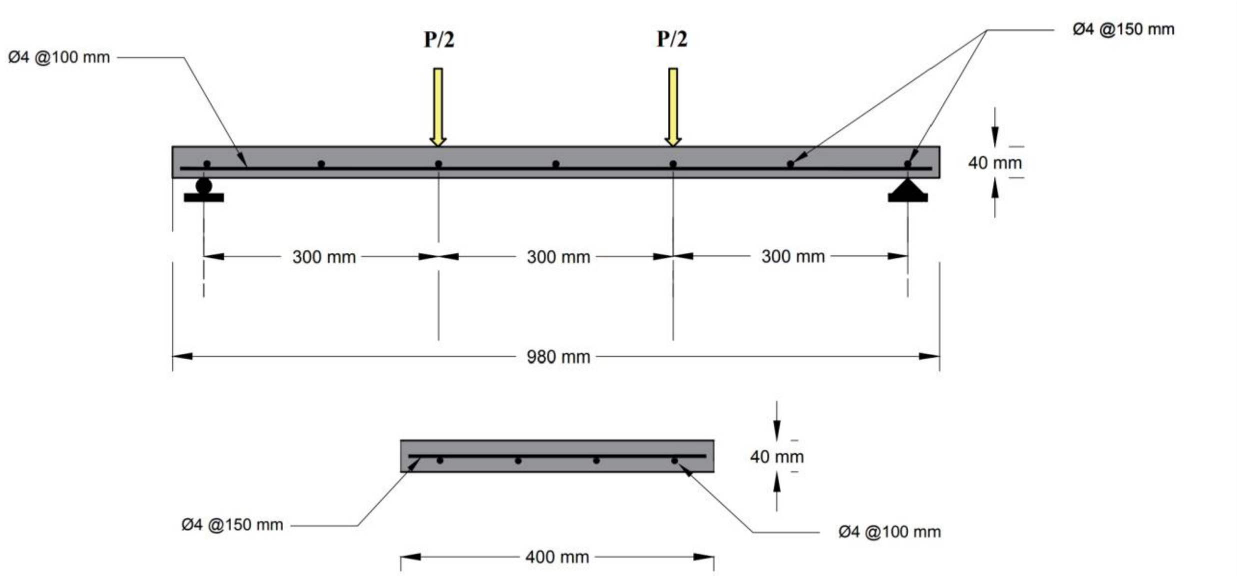


**Figure 1.** Details of longitudinal and cross-section of control specimen

*2.3. Concrete mixes*

Five mixes of RPC were adopted in the present investigation, more than mix proportion was attempted to obtain a highest compressive strength with flow equal to 95% in accordance with ASTM C1437 [30]. The proportions of materials in these mixes are shown in Table 6. Mixes included two variables: the volumetric percentage of steel fiber (adopted three proportions: 0, 1, and 2%) and the content of silica fume (adopted three proportions: 15, 20, and 25%). The best mix that gave the greatest results consisted of 1cement: 1sand: 0.25silica fume: 0.2water-cement ratio w/c and water to binder proportion w/b equal to 0.16, in addition, the superplasticizer was 7% of the cementitious mix. The optimum compressive strength obtained from the mixes was 121 MPa at age of 28 days, which achieved good workability and consistency for this concrete mixture without being segregation and adopted to cast all tested slabs and their control specimens (cylinders and prisms).

### *2.4. Mixing procedure*

All the mixing of reactive powder concrete was executed in a horizontal rotary mixer of capacity equal to 0.1 $m^3$. Cement, in addition to silica fume, was mixed in a dry state for 3 minutes to ensure uniform distribution of the powder of silica fume with the particles of cement. Thereafter, the required quantity of fine aggregate was placed into the mixer, and this process continued for five minutes. Then, water and superplasticizer were stirred, and the solution was gradually inserted into the mixture for a sufficient time. The process of mixing was paused to move the ingredients by hand; thereafter, the operation continued for three minutes. The last phase was returned three times to ensure the mixture became homogeneous. After that, steel fibers were slowly added into the mixture by hand for three minutes. The overall time of mixing was about 25–30 minutes.

**Table 6:** RPC mixes types

| Mix Type | Cement kg/$m^3$ | Sand kg/$m^3$ | Steel Fibers* % | Steel Fibers kg/$m^3$ | Silica Fume** % | Silica Fume kg/$m^3$ | S.P.*** % | Flow % | w/c |
|---|---|---|---|---|---|---|---|---|---|
| M0,25 | 1000 | 1000 | 0 | 0 | 25 | 250 | 7 | 95 | 0.2 |
| M1,25 | 1000 | 1000 | 1 | 78 | 25 | 250 | 7 | 85 | 0.2 |
| M2,25 | 1000 | 1000 | 2 | 156 | 25 | 250 | 7 | 75 | 0.2 |
| M2,15 | 1000 | 1000 | 2 | 156 | 15 | 150 | 7 | 85 | 0.2 |
| M2,20 | 1000 | 1000 | 2 | 156 | 20 | 200 | 7 | 80 | 0.2 |

* Percent of mix volume.

** Percent of the weight of cement.

*** Superplasticizer which be as percent of weight of binder (cement + silica fume).

### *2.5. Determination of workability and consistency of the mixtures of concrete*

The flow table test is the method used to determine the consistency of RPC mixes before casting concrete into molds. Flow is recognized by the resulting increase in the mean diameter of the mortar mass base, represented by a percentage of the original diameter of the test cone base as shown in Figure 2. For all mix types of concrete, workability was determined using a flow table test identical to that indicated in ASTM C1437 [30] and ASTM C230-83 [31] specifications.

$$Flow = \frac{(D-100)}{100} X100\%$$

D: The mean diameter of the distributed concrete (mm), measured in four positions. Table 6 shows the mixes whose range of flow lies between the value of 75% and the value of 95%.

**Figure 2.** Flow table test

### *2.6. Mechanical properties of hardened RPC*

#### *2.6.1. Compressive strength*

The important property of concrete is compressive strength. Its test is done confirms with ASTM C39 requirements [32] on cylinders of 100x200 mm utilizing a digital hydraulic machine with capacity of 2000 KN. Average of 3 cylinders was adopted to get mean compressive strength for concrete mix. All specimens were tested at the age of 28 days.

#### *2.6.2. Splitting tensile strength*

Splitting tensile strength tests were done on concrete cylinders measuring 100x200mm according to ASTM C496-04 [33]. The load applied continuously on each specimen until failure utilizing a digital hydraulic machine with capacity of 2000 KN. Average of 3 cylinders was adopted to get mean splitting strength for concrete mix. All specimens were tested at the age of 28 days.

#### *2.6.3. Modulus of rupture*

Modulus of rupture tests were done on concrete prisms measuring 100x100x500mm. A simply supported prism with a clear span of 300mm was tested up to failure in a digital hydraulic machine with a capacity of 2000 KN. The load applied to prisms at two-point, according to ASTM-C78-02 [34]. The average of 3 prisms was adopted to get the mean modulus of rupture for each mix. All specimens were tested at the age of 28 days.

### *2.7. Casting procedure and curing*

All the forms of slabs and the molds of specimens were fixed, cleaned completely, and oiled. For slabs, the steel reinforcement was placed in the right place. Then, concrete mixes were placed into all specimen molds in the form of layers with vibrating. The vibration process continued for a sufficient time until most of the air voids were removed, then the surfaces of the molds were levelled and finished well by using a steel trowel. The plastic nylon sheets were put over the specimens to protect them from evaporation and retain moisture until the ultimate setting occurred. After 24 hours, the cast specimens (slabs, cylinders, and prisms) were taken out of their forms and marked, then put in a tank full of water for 27 days. All specimens were cured and tested under laboratory conditions. As curing period is finished, taken all specimens out the tanks of water and stored in the lab until the testing date.

## 3.Results and discussion

### *3.1. Mechanical properties of hardened RPC*

#### *3.1.1. Compressive strength*

The test results shown in Table 7 revealed that the concrete that contained steel fiber displayed ductile behavior at failure, while the concrete without steel fiber failed in a brittle and explosive behavior at failure. An increase in the steel fiber volumetric ratio in concrete specimens from 0% to 1% and then to 2% resulted in increasing the average compressive strength by 41.79% and 80.59%, respectively. The results of Table 7 demonstrated that the compressive strength increased due to increased silica fume. As the proportion of silica fume in concrete specimens increased from 15% to 20% and to 25%, the test results of compressive strength increased by 14.43% and 24.74% respectively. This behavior is attributable to particle packing when the particles of silica fume fill the spaces between cement particles additionally from densified chemical reactions because of the pozzolanic reaction and silica hydrate transformation.

#### *3.1.2. Splitting tensile strength*

The results revealed that when the steel fiber volumetric ratio in concrete specimens increased from 0% to 1% and then to 2%, the average splitting strength increased by 87.28% and 160.87% respectively, as shown in Table 7. From the previous results, it can be observed that there is a largely steel fiber effect on RPC tensile strength. This is attributed to the bridge tensile cracks and the slow propagation of cracks by using steel fiber. The results of Table 7 revealed that when the silica fume proportion in concrete specimens increased from 15% to 20% and then to 25%, the test results of splitting tensile strength increased by 8.24% and 16.13%, respectively. These results indicate that the effect of silica fume was small compared with the steel fiber effect on increasing splitting tensile.

### *3.1.3. Modulus of rupture*

The results of Table 7 demonstrated that steel fiber percentage has a largely positive impact on increasing the magnitude of the modulus of rupture for concrete specimens. It was noticed that when steel fiber percentage increased from 0% to 1% and then to 2%, modulus of rupture magnitude increased by 115.41% and 243.42%, respectively. While silica fume impact on the modulus of rupture was slight, the results of Table 7 showed that as the silica fume proportion increased from 15% to 20% and then to 25%, there was an increase in the modulus of rupture of 13.85% and 19.33%, respectively.

**Table 7:** Mechanical properties for mixes used in this research

| Mix Type | Compressive Strength ($f_c'$) | Splitting Tensile Strength ($f_{ct}$) | Modulus of Rupture ($f_r$) |
|---|---|---|---|
| M0,25 | 67 MPa (0%) | 6.21 MPa (0%) | 5.32 MPa (0%) |
| M1,25 | 95 MPa (41.79%) | 11.63 MPa (87.28%) | 11.46 MPa (115.41%) |
| M2,25 | 121 MPa (80.59%)<br>(24.74%) | 16.2 MPa (160.87%)<br>(16.13%) | 18.27 MPa (243.42%)<br>(19.33%) |
| M2,15 | 97 MPa (0%) | 13.95 MPa (0%) | 15.31 MPa (0%) |
| M2,20 | 111 MPa (14.43%) | 15.1 MPa (8.24%) | 17.43 MPa (13.85%) |

**Figure 3.** Specimens of concrete properties tests

### *3.2. Flexural tests of the slabs*

Five slabs were tested beyond casting by 28 days. Slabs painted a white color to make it easy to observe the cracks. The slabs were tested by applying two-line loads using a digital hydraulic machine with a capacity of 600 kN, which exists in the structural lab of the engineering college at the University of Diyala. The specimens were supported at the edges in a simply supported case with a clear span of 900mm. The loads were gradually applied at a rate of loading 0.25 MPa/s until the specimens reached failure. The mid-span deflection was determined by using an LVDT sensor and fixed under the lower face of the tested slabs. Figure 4 shows a slab under testing. The effect of two parameters on the flexural behavior of RPC one-way slabs was studied. First parameter was the impact of changing steel reinforcement percentages in the slabs, and second parameter was the impact of using different thicknesses in the slabs. During the application of loads, first cracking load, the ultimate test load, and deflection in mid-span were recorded.


**Figure 4.** Slab under testing

#### *3.2.1. Effect of steel reinforcement ratios on structural behavior of slabs*

Three reactive powder reinforced concrete one-way slabs (1, 2, and 3) were cast and tested to investigate the impact of utilizing different proportions of steel reinforcement on the flexural performance of RPC one-way slabs. These slabs contain a reinforcement ratio of 0.36%( Ø 4 mm @ 150 mm c/c), 0.48%( Ø 4 mm @ 100 mm c/c), and 0.60%( Ø 4 mm @ 75 mm c/c) with using steel fiber proportion of 2%, silica fume percentage of 25% (mix type: M2,25) and slab thickness of 40 mm. Table 8 demonstrates the impact of steel reinforcement percentage on first crack load, the ultimate test load, and ultimate deflection in the mid-span of test slabs (S1, S2, and S3). As steel reinforcement proportion increased from a magnitude of 0.36% to 0.48% and then to 0.60%, the first cracking load increased from a value of 4.2 kN to a value of 5 kN and to 6 kN with an increasing percentage of 19.05% and 42.86%, respectively. Also, the ultimate flexural load increased from 11kN to 13.31 kN and 15.5 kN with an increasing percentage of 21% and 40.91%, respectively, and the deflection increased from 23.29 mm to 27.43 mm and then to 30.04 mm with an increasing percentage of 17.78% and 28.98%, respectively. At the loading start, the emerging stresses in the tested slabs were carried out by concrete, and the tension zone did not contain any cracks. Flexural cracks began to appear in the area between two-point loads where the tensile stresses exist and exceed the specified tensile strength of concrete, and at this stage, the load was named first cracking load. By increasing load that applied on specimens, the cracks propagate more, and their width is expanded until failure. Load-deflection curves for the tested slabs are demonstrated in Figure 5**,** which shows that at the start of loading, the relationship between loads and deflection is closely linear, without any emerging cracks. After that, by increasing the applied load, the cracks have been occurred at the lower face of the slabs in the area surrounding the two applied loads, where the maximum flexural moment occurred. First cracking load, maximum deflection in the central span of slabs, and ultimate test load were increased due to the increase in steel reinforcement percentage. This behavior is attributed to increasing the tensile strength of slabs due to increasing the proportion of steel reinforcement, which subsequently increases the slab's ability to resist external loads that cause tension, such as bending loads. In addition, increasing the proportion of steel reinforcement results in increased bearing capacity of the slabs, where the slabs can resist greater loads before breaking or collapsing, and also increased bending energy, where the slabs have a greater ability to absorb bending energy before failure occurs. Also from these curves, it can also be observed that the deflection decreases with an increase in the proportion of steel reinforcement at the same value of load, which belongs to the fact that an increasing proportion of steel reinforcement improves the control of cracks and stops the bending cracks from further widening, additionally, increasing the proportion of steel reinforcement results in increased slab rigidity, where the slab becomes more solid and able to resist deformation. The slope of the curves became less and continued to minimize gradually till the steel reached the yielding stage, which confirms that the increasing ratio of steel reinforcement in RPC one-way slabs results in increased flexural stiffness. After the reinforcements yielded, the strain hardening happened, and a small increase in applied loads led to a high increment in mid-span deflection until the slab reached failure.

**Table 8:** Impact of steel reinforcement proportions on slabs experimental test results

| Slab No. | Mixes | Steel rein. ratio (%) | $P_{cr}$ KN | $(P_{cr} - P_{cr\,S1})/P_{crS1} \times 100$ | $P_{ult}$ KN | $(P_{ult} - P_{ult\,S1})/P_{ult\,S1} \times 100$ | $\Delta_{max}$ mm | $(\Delta_{max} - \Delta_{max\,S1})/\Delta_{max\,S1} \times 100$ |
|---|---|---|---|---|---|---|---|---|
| 1 | M2,25 | 0.36 | 4.2 | 0 | 11 | 0 | 23.29 | 0 |
| 2 | M2,25 | 0.48 | 5 | 19.05 | 13.31 | 21 | 27.43 | 17.78 |
| 3 | M2,25 | 0.60 | 6 | 42.86 | 15.5 | 40.91 | 30.04 | 28.98 |

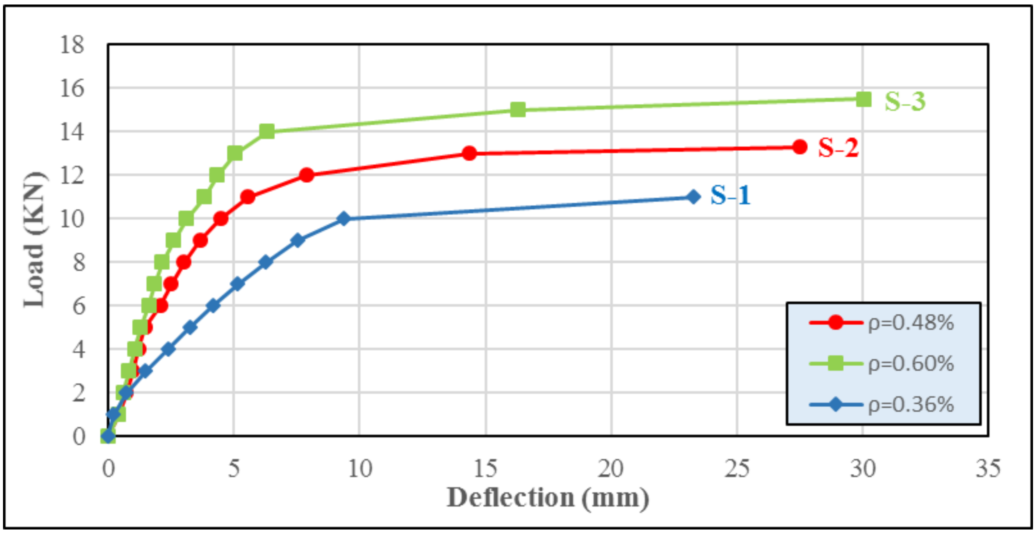


**Figure 5.** Impact of steel reinforcement proportions on relation between load and deflection RPC slabs

*3.2.2. Effect of slab thickness on structural behavior of slabs*

Three reactive powder reinforced concrete one-way slabs (2, 4, and 5) were cast and tested to investigate the impact of utilizing varying values of slab thickness (40mm, 60mm, and 80mm) on the flexural behavior of RPC one-way slabs. These slabs contain 0.48% steel reinforcement, steel fiber with a percentage of 2%, and silica fume with a percentage of 25%. Table 9 shows the slab thickness effect on the first cracking load, ultimate test load, and maximum deflection in the central span of slabs (S2, S4, and S5). When slab thickness increased from a value of 40mm to a value of 60mm and then to 80mm, the first cracking load increased from 5 kN to 13.3 kN and to 17 kN with an increasing percentage of 166% and 240%, respectively. Also, for the same increase in slab thickness, the ultimate flexural load increased from 13.31 kN to 27.16 kN and then to 44.55 kN with an increasing percentage of 104.06% and 234.71%, respectively, and the ultimate deflection decreased from 27.43mm to 17.33mm and then to 11.45mm with a decreasing percentage of 36.82% and 58.26%, respectively. Increasing slab thickness resulted in an overall decrease in the density of cracks and an increase in crack width due to increasing the tensile strength of the slab. The relationship between loads and mid-span deflection for tested RPC one-way slabs by utilizing different thicknesses of slabs is demonstrated in Figure 6. It was observed that slab thickness increases lead to an increase in the load that causes appearance of a first crack, the ultimate load that slabs could carry out, and a decrease in the ultimate mid-span deflection. This behavior is achieved by crack control, where the ability of RPC slabs to resist the formation and propagation of cracks increases due to increased slab thickness, so that slabs with a greater cross section can potentially develop wider cracks and carry out higher tension and compression loads than slabs with a smaller cross section, which are more prone to developing cracks at lower loads. Additionally, as slab thickness increased, the moment of inertia of the slab section increased, resulting in greater capacity to carry bending loads, allowing slabs to support higher loads before failure. The deflection in the central span of the slab decreases due to increased slab thickness, so that the slabs with greater thickness deflect less than the slabs with smaller thickness. This behavior is attributed to the increased stiffness of thicker slabs compared to thinner slabs.

**Table 9:** Impact of slab thickness on slabs experimental test results

| Slab No. | Mixes | Slab thickness (mm) | $P_{cr}$ KN | $(P_{cr} - P_{cr\,S2})/P_{crS2} \times 100$ | $P_{ult}$ KN | $(P_{ult} - P_{ult\,S2})/P_{ult\,S2} \times 100$ | $\Delta_{max}$ mm | $(\Delta_{max} - \Delta_{max\,S2})/\Delta_{max\,S2} \times 100$ |
|---|---|---|---|---|---|---|---|---|
| 2 | M2,25 | 40 | 5 | 0 | 13.31 | 0 | 27.43 | 0 |
| 4 | M2,25 | 60 | 13.3 | 166 | 27.16 | 104.06 | 17.33 | -36.82 |
| 5 | M2,25 | 80 | 17 | 240 | 44.55 | 234.71 | 11.45 | -58.26 |

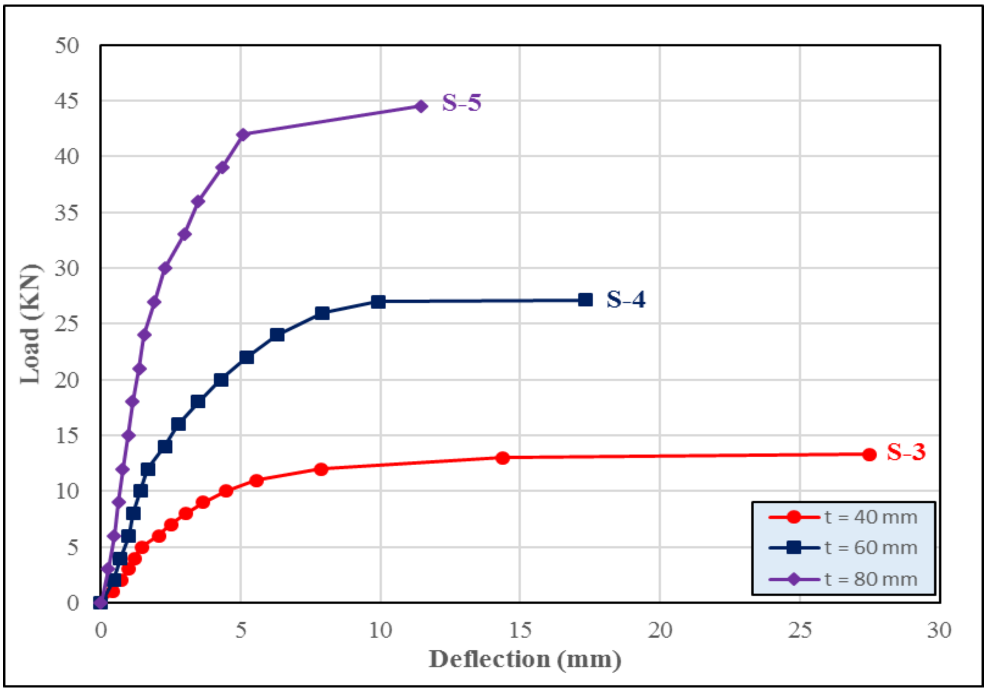


**Figure 6.** Impact of slab thickness on relation between load and deflection RPC Slabs

### *3.2.3. Crack patterns and failure modes*

Slabs that have been cast and then tested in this investigation were five. These slabs were divided into two groups: the first were similar in all properties except steel reinforcement proportion, and the second were similar in all properties except slab thickness; hence, crack patterns, ultimate loads, and modes of failure were different. In reinforced concrete slabs, cracks are created in the places where the principal tensile stresses occur and overtake the concrete's specified tensile strength. First cracks in the slabs appeared at the bottom surface and were parallel to the direction of the two concentrated line loads. A lot of vertical cracks developed in the zone between two-line loads as loads were increased, and the failure became faster before it reached the ultimate capacity. All the tested slabs of this investigation failed in pure bending, with one major crack and many minor cracks in the middle third region, where the value of the bending stresses is the maximum, which caused the creation of cracking through the tension region. Steel reinforcement percentage effect was significant on the pattern of cracking and can be observed in slab failure, where increasing the proportion of steel reinforcement in the tested slabs resulted in an overall decrease in the density of cracks and crack width due to increasing the tensile strength of the slabs. The number of cracks that appeared on slabs with a higher proportion of steel reinforcement (0.60% in slab S3) was less than those that appeared on slabs with a lower steel reinforcement ratio (0.36% in slab S1) and (0.48% in slab S2). Also, the cracks in slab S3 were narrow and distributed over a limited area of the slab compared with slabs S1 and S2. This behavior is attributed to the increased steel reinforcement in the section, The cracks in slabs S1 and S2 were mainly perpendicular to the direction of the longitudinal reinforcement bars, and as the proportion of steel reinforcement increases in slab S3, the cracks begin to deviate from the direction of the reinforcement and become more inclined. As demonstrated in Figure 7, which shows the tested slabs crack patterns after their failure.

Slab thickness effect on the pattern of cracking can be seen in the failure of slabs. Increasing slab thickness resulted in an overall decrease in the density of cracks and an increase in crack width due to increasing the tensile strength of the slab, where slab S5 with a thickness of 80mm has limited and wider cracks compared with slabs S2 with a thickness of 40mm and S4 with a thickness of 60mm, which have more cracks and narrower cracks. This behaviour belongs to increasing the ability of RPC slabs to resist the formation and propagation of cracks due to increasing slab thickness. Thicker slabs with a great cross section can potentially develop wider cracks, but they tend to be less numerous due to the greater concrete volume resisting them, while thinner slabs with a smaller cross section are more prone to developing cracks at a lower load. These cracks were finer, but they are more numerous due to the reduced concrete resisting them. The cracks in slabs S2 and S4 were mainly perpendicular to the direction of the longitudinal reinforcement bars, and as slab thickness increases in slab S5, the cracks begin to deviate from the direction of the reinforcement and become more inclined. Also, some of the cracks that emerged in slab S5 were continuous along the slab width, while all the cracks that emerged in slabs S2 and S4 were not continuous and widespread over the cracking area between two applied loads, as demonstrated in Figure 8, which shows the tested slabs crack patterns after their failure.

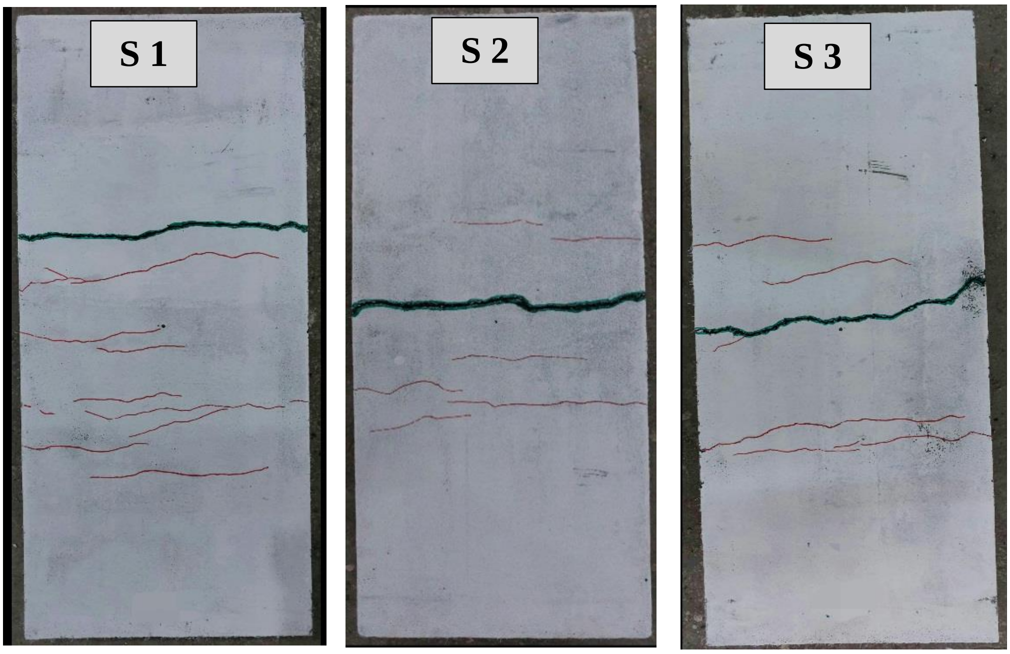


**Figure 7.** Impact of steel reinforcement proportion on crack pattern

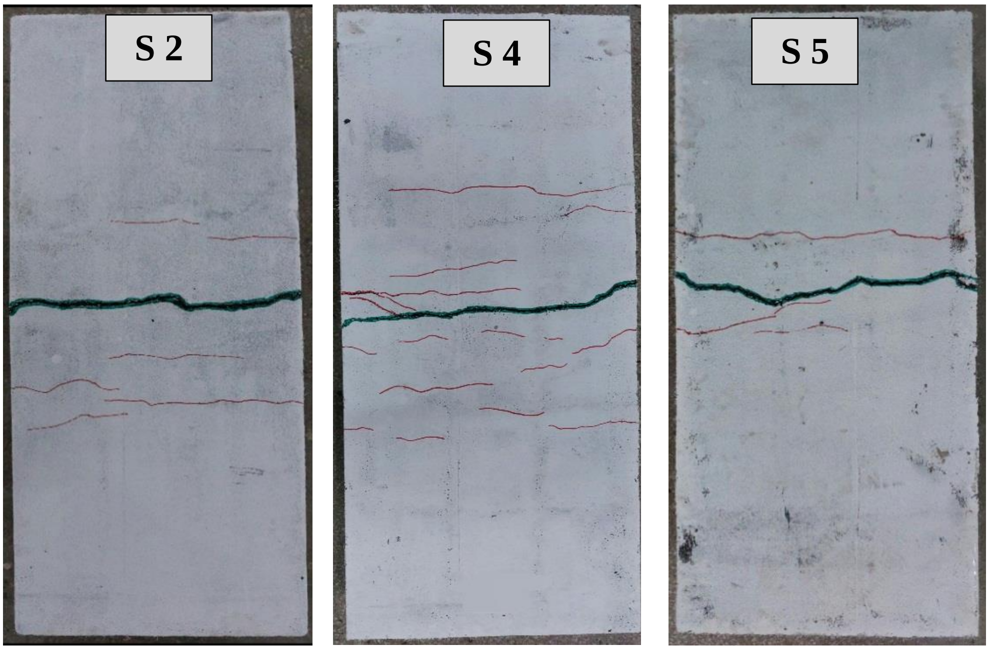


**Figure 8.** Impact of slab thickness on crack pattern

## 4. Conclusions

Depended on the results of the experimental work, the most important conclusion reached in this investigation is:

1. Experimental work revealed an increase in the compressive strength of the specimens due to an increase in steel fiber and silica fume proportions.
2. Utilizing silica fume and steel fiber in the mixes of RPC increased splitting tensile strength.
3. Modulus of rupture of RPC prisms increased when each of the steel fiber percentages and silica fume proportions increased.
4. All the slabs tested in the present investigation failed flexural tension by one major crack and many minor cracks distributed on the slabs lower face in the area between two-line loads.
5. Increasing the proportion of steel reinforcement in the tested slabs resulted in an overall decrease in the density of cracks and crack width due to increasing the tensile strength of the slabs. The cracks in slabs with less steel reinforcement proportion were mainly perpendicular to the direction of the longitudinal reinforcement bars, while the cracks in slabs with more steel reinforcement proportion began to deviate from the direction of the reinforcement and become more inclined.
6. Increasing slab thickness resulted in an overall decrease in the density of cracks and an increase in crack width due to increasing the tensile strength of the slab. The cracks in thinner slabs were mainly perpendicular to the direction of the longitudinal reinforcement bars, while the cracks in thicker slabs began to deviate from the direction of the reinforcement and become more inclined. Some of the cracks that emerged in thicker slabs were continuous along the slab width, while all the cracks that emerged in thinner slabs were not continuous and widespread over the cracking area between two applied loads.
7. Flexural tests of slabs revealed that an increase in the ultimate test load and the first crack load were due to an increase in the proportion of steel reinforcement, where increasing the steel reinforcement proportion enhances crack control and prevents the bending cracks from further

widening. As the steel reinforcement proportion increased from the value of 0.36% to 0.48% and then to 0.60%, the first cracking load increased with a percentage of 19.05% and 42.86%, respectively, and the ultimate load increased with a percentage of 21% and 40.91%, respectively.

8. The impact of slab thickness on the first cracking load and the ultimate load of a one-way slab is significant; when slab thickness increased from 40mm to 60mm and then to 80mm, the first crack load increased by a percent (166% and 240%), respectively, and the ultimate load increased by a percentage (104.06% and 234.71%), respectively. This behavior is attributed to the control of cracks, where the ability of slabs to resist the formation and propagation of cracks increases due to increased slab thickness, so that slabs with a greater thickness can potentially develop wider cracks and carryout higher tension and compression loads than slabs with a smaller thickness.
9. Increasing steel reinforcement proportions improves the ductility of tested specimens and increases ultimate mid-span deflection. When the steel reinforcement proportion was increased from 0.36% to 0.48% and then to 0.60%, the increasing percentage of ultimate mid-span deflection was 17.78% and 28.98%, respectively.
10. Increasing slab thickness results in decreased ultimate mid-span deflection. When slab thickness was increased from 40mm to 60mm and then to 80mm, the decreasing percentage of ultimate mid-span deflection was 36.82% and 58.26%, respectively. This behavior is attributed to the increased stiffness of thicker slabs compared to thinner slabs.

## References


[1] P. Richard and M. H. Cheyrezy, "Reactive powder concretes with high ductility and 200-800 MPa compressive strength," *Special Publication,* vol. 144, pp. 507-518, 1994.

[2] S. Collepardi, L. Coppola, R. Troli, and M. Collepardi, "Mechanical properties of modified reactive powder concrete," *ACI Special Publications,* vol. 173, pp. 1-22, 1997.

[3] P. Richard and M. Cheyrezy, "Composition of reactive powder concretes," *Cement and concrete research,* vol. 25, no. 7, pp. 1501-1511, 1995.

[4] A. Al-Tikrite and M. N. Hadi, "Mechanical properties of reactive powder concrete containing industrial and waste steel fibres at different ratios under compression," *Construction and Building Materials,* vol. 154, pp. 1024-1034, 2017.

[5] L. S. Danha, W. I. Khalil, and H. M. Al-Hassani, "Mechanical properties of reactive powder concrete (RPC) with Various Steel Fiber and Silica Fume Contents," *Engineering and Technology Journal,* vol. 31, no. 16, pp. 3090-3108, 2013.

[6] P. Y. Blais and M. Couture, "PRECAST, prestressed pedestrian BRIDGE-WORLD'S first reactive powder concrete bridge," *PCI journal,* vol. 44, no. 5, 1999.

[7] C. R. Michaluk, S. H. Rizkalla, G. Tadros, and B. Benmokrane, "Flexural behavior of one-way concrete slabs reinforced by fiber reinforced plastic reinforcements," *ACI structural Journal,* vol. 95, pp. 353-365, 1998.

[8] B. Zhang, R. Masmoudi, and B. Benmokrane, "Behaviour of one-way concrete slabs reinforced with CFRP grid reinforcements," *Construction and Building Materials,* vol. 18, no. 8, pp. 625-635, 2004.

[9] L. Ombres, T. Alkhrdaji, and A. Nanni, "Flexural analysis of one way concrete slabs reinforced with GFRP rebars," in *International meeting on composite materials, PLAST,* 2000, pp. 243-250: Citeseer.

[10] K. Chang and D. Seo, "Behavior of one-way concrete slabs reinforced with GFRP bars," *Journal of Asian Architecture and Building Engineering,* vol. 11, no. 2, pp. 351-358, 2012.

[11] Z. R. Aljazaeri and J. J. Myers, "Flexure performance of RC one-way slabs strengthened with composite materials," *Journal of Materials in Civil Engineering,* vol. 30, no. 7, p. 04018120, 2018.

[12] D.-Y. Yoo and Y.-S. Yoon, "Influence of steel fibers and fiber-reinforced polymers on the impact resistance of one-way concrete slabs," *Journal of Composite Materials,* vol. 48, no. 6, pp. 695-706, 2014.

[13] H. M. Elsanadedy, T. H. Almusallam, S. H. Alsayed, and Y. A. Al-salloum, "Experimental and FE study on RC one-way slabs upgraded with FRP composites," *KSCE Journal of Civil Engineering,* vol. 19, pp. 1024-1040, 2015.

[14] A. A. Allawi and H. A. Jabir, "Experimental behavior of laced reinforced concrete one way slab under static load," *Journal of Engineering,* vol. 22, no. 5, pp. 42-59, 2016.

[15] M. Adom-Asamoah and C. K. Kankam, "Flexural behaviour of one-way concrete slabs reinforced with

steel bars milled from scrap metals," *Materials & Design*, vol. 30, no. 5, pp. 1737-1742, 2009.
[16] A. Baarimah and S. S. Mohsin, "Behaviour of reinforced concrete slabs with steel fibers," in *IOP Conference Series: Materials Science and Engineering*, 2017, vol. 271, no. 1, p. 012099: IOP Publishing.
[17] T. G. Kumari, C. Puttappa, C. Shashidar, and K. Muthu, "Flexural Characteristics of SFRSCC and SFRNC one way slabs," *IJRET: International Journal of Research in Engineering and Technology*, pp. 2321-7308, 2013.
[18] Q. W. Ahmed, "Strength and behavior of reinforced concrete one-way slabs with opening in flexural," in *2018 1st International Scientific Conference of Engineering Sciences-3rd Scientific Conference of Engineering Science (ISCES)*, 2018, pp. 293-298: IEEE.
[19] M. Gurutzeaga, E. Oller, C. Ribas, A. Cladera, and A. Marí, "Influence of the longitudinal reinforcement on the shear strength of one-way concrete slabs," *Materials and structures*, vol. 48, pp. 2597-2612, 2015.
[20] E. O. Lantsoght, C. Van Der Veen, and J. C. Walraven, "Shear in one-way slabs under concentrated load close to support," *ACI Structural Journal*, vol. 110, no. 2, p. 275, 2013.
[21] O. A. Qasim, "Behavior of reinforced reactive powder concrete slabs with openings," PHD. Thesis, AL-Nahrain University College of Engineering, Civil Engineering …, 2013.
[22] A. A. Alfeehan, H. I. Abdulkareem, and S. H. Mutashar, "Flexural behavior of sustainable reactive powder concrete bubbled slab flooring elements," *Challenge Journal of Structural Mechanics*, vol. 3, no. 2, pp. 81-89, 2017.
[23] Y. G. Abtan and H. F. Hassan, "Flexural Strength of Modified Reactive Powder Concrete One Way Slabs," *The Open Civil Engineering Journal*, vol. 13, no. 1, 2019.
[24] Iraqi specification, No.5/2019., “Portland cement”.
[25] Iraqi Specification, No. 45/1984, “Aggregate from Natural Sources for Concrete and Construction”.
[26] ASTM C1240-04, “Standard Specification for the Use of Silica Fume as a Mineral Admixture in Hydraulic Cement Concrete, Mortar and Grout”, Vol. 4.2, 2004, 6p.
[27] ASTM C 494/C 494M-1999a, "Standard Specification for Chemical Admixtures for Concrete", Vol. 04.02, 1999, pp.1-9.
[28] ASTM A820/A 820M-2004, "Standard Specification for Steel Fiber for Fiber-Reinforced Concrete", 2004, pp.1-4.
[29] ASTM A615/615M-05a, (2005),"Standard Specification for Deformed and Plain Carbon Structural Steel Bars for Concrete Reinforcement", ASTM Standards, Vol.01.02, 6p.
[30] ASTM C1437-2001, "Standard Test Method for Flow of Hydraulic Cement Pastes and Mortars of Plastic Consistency", Vol. 04.01, 1999, 3p.
[31] ASTM C230-83, "Standard Specification for Flow Table for use in Tests of Hydraulic Cement", Annual book of ASTM standards, vol. 04.02, 1983. 163-168.
[32] ASTM C39/C39M-05, "Standard Test Method for Compressive Strength of Cylindrical Test Specimens", Vol. 04.02, 2003.
[33] ASTM C496/C496M-04, "Standard Test Method for Splitting Tensile Strength of Cylindrical Concrete Specimens", Vol. 04.02, 2004, 5p.
[34] ASTM C78-02, (2002) ,"Standard Test Method for Flexural Strength of Concrete(Using Simple Beam with Third-Point Loading", ASTM Standard, Vol. 04.02, 3p.